

Influence of the Cross-Section Form of the Power Bus Bar on its Parameters

S. Ternov, A.V. Demakov, M.E. Komnatnov, *Member, IEEE*

Abstract—Per-unit-length inductance and characteristic impedance are the main parameters that affect the operation of power bus bar (PBB). When designing the PBB there are attempts to reduce these parameters in various ways. The cross-section size and the material of dielectric have a significant influence on the parasitic parameters of the PBB. In this paper, we calculate the line parameters of PBB for various values of dielectric permittivity and cross-sectional shapes (for the constant area of 50 mm²). The results of calculations of the PBB parameters with the change of the thickness, width, and shape of the conductors are presented. The analysis of the mass, dimensions and technological possibilities of PBB manufacturing is carried out. The optimal parameters of the cross-section of PBB were determined according to the criteria of the minimum per-unit-length inductance and the characteristic impedance.

Keywords— electromagnetic compatibility, bus bar, S-parameters, power supply, parasitic parameters, parasitic inductance, impedance

I. INTRODUCTION

In power electronics, the PBBs are used to reduce the influence of parasitic parameters of electrical connections between the source and the consumer. Parasitic parameters can lead to unstable operation of active elements due to overvoltage, voltage drops, currents imbalance, resonance in capacitors and etc. [1, 2]. The use of modern active elements in power converters increases the efficiency of the device achieved in several ways, one of which is an increase in switching frequencies [3]. The estimation of the conductive and radiated electromagnetic interference of the PBB can be performed on the basis of a simple approach based on analytical formulas and modelling with the calculation of the waveform and the magnitude of the magnetic field [4]. Also, parasitic parameters are extracted for estimating conductive interference, using the partial element equivalent (PEEC) method [5, 6]. To reduce the induced interference, the coupled capacitance method is used, which involves the alternation of the ground layers, thereby absorbing voltage surges [7]. Also, the various integrated filters [8] and various methods of reducing the parasitic inductive coupling and the characteristic impedance of the PBB are used, which allows the converters to operate at higher frequencies [9]. A design of low-

inductance PBB is developed which allows reducing the voltage dips in power inverter modules [10].

Estimation of correct values of parasitic parameters can turn out to be a rather laborious process since it is necessary to find the optimal solution between parasitic parameters, thermal properties, and mass and dimensions of the structure. For simple PBB designs, analytical parameter estimation [11] or an estimation based on PEEC [12] is used. Full-wave modelling and optimization of PBB are performed using the finite element method (FEM) [13], and also modelling with combined electric and thermal numerical models to calculate the spatial distribution of electrical and thermal quantities [14–16]. The constructive features of the interrelationship between the geometry of PBB and its electrical and physical parameters remain a promising line of research for optimizing. So, for example, many different solutions are compared, the influence of the external form is considered and on their basis, the recommended guideline for PBB's designing are proposed [17]. The advantage of a circular form of cross-section as compared to rectangular form was demonstrated. The coaxial construction of the PBB is obtained from a set of N tubes. A feature of this design is the absence of a resulting magnetic field in the environment of PBB, as well as low values of the elements of the inductance matrix, low power losses, high mechanical stability in the case of short-circuit currents and low influence of the eddy current and proximity effect [18].

From the foregoing, it follows that the shape of the cross-section, the materials of the conductors and dielectrics exert a special influence on the parameters of the PBB. Therefore, the aim of this paper is to investigate the influence of the shape of the cross-section of the PBB on its parameters.

II. RECTANGULAR CROSS-SECTION OF BUS BAR

A. Increasing of conducting width

The initial geometric parameters of the cross-section of the PBB were taken from the design considered in [19]. For conductors of PBB with width w , thickness t and $S=w \times t=50$ mm², the approximate maximum power is 19 kW for DC circuits according to

$$P = \frac{U \cdot w \cdot t}{258 \cdot 10^{-9}}. \quad (1)$$

The quasi-static models were created, and analysis of the cross-sections of the PBB in the TALGAT system was performed [20]. The first model (Fig. 1a) consists of two parallel metal plates with the width $w = 10$ mm and thickness $t_1 = 5$ mm, between which there is a dielectric with $\epsilon_r = 4.3$ and thickness $t_2 = 2$ mm. The second model (Fig. 1b) has an

This research was supported by The Ministry of Education and Science of the Russian Federation (RFMEFI57417X0172)

S. Ternov, A. V. Demakov and M. E. Komnatnov are with Department of Television and Control, Tomsk State University of Control Systems and Radioelectronics, Tomsk, Russian Federation (e-mail: stanislav.1995@mail.ru, vandervals@inbox.ru, maxmek@mail.ru).

additional insulation obtained by oxidizing the conductor ($t_3=50 \mu\text{m}$, $\epsilon_r=20$), by covering with the EP-730 lacquer ($t_4=18\text{--}20 \mu\text{m}$, $\epsilon_r=4$) and winding a film ($t_5=200 \mu\text{m}$, $\epsilon_r=2.3$).

The calculation of the per-unit-length inductance L and the capacitance C was performed for the first and second models of the PBB with a change in the parameters w (from 100 mm to 10 mm) and t_1 (from 0.5 mm to 5 mm) with a constant cross-section area $S=50 \text{ mm}^2$. The width w of the dielectric varies in the same way as in the conductor, and its thickness t_2 does not change. Also, the thickness t_3 , t_4 , t_5 of additional dielectric materials remained unchanged.

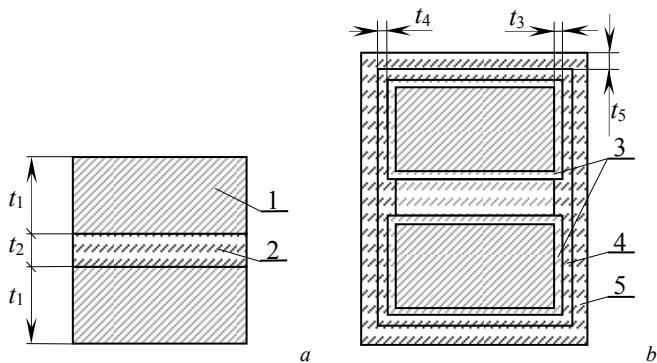


Fig. 1. The cross-section of PBB: initial (a) and complemented (b) models consisting of a metal (1) and dielectrics with different ϵ_r ($\epsilon_r=4.3$ (2), $\epsilon_r=20$ (3), $\epsilon_r=4$ (4), $\epsilon_r=2.3$ (5))

The L and C values (Fig. 2) and characteristic impedance Z (Fig. 3) for PBB are obtained as a function of the aspect ratio w/t_1 of the cross-section.

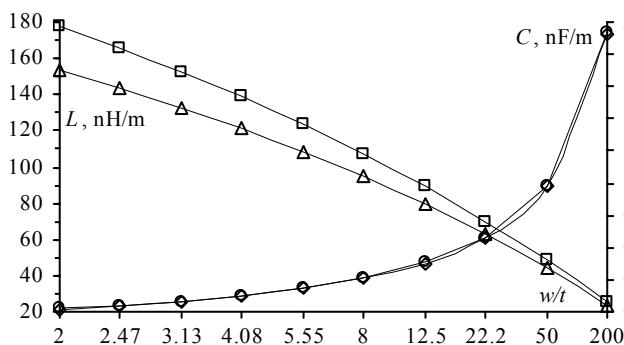


Fig. 2. The values of the per-unit-length inductance L and the capacitance C , depending on the variation in the aspect ratio w/t_1 for the two models of the PBB with the cross-sectional area $S=50 \text{ mm}^2$ without (a) (Δ, \diamond) and with additional dielectric materials (b) (\square, \circ)

Fig. 2 shows that with an increase in w/t_1 from 2 to 200, the L values decreased from 177.3 nH/m to 23.3 nH/m, and the value of C increased from 217.5 pF/m to 1937.6 pF/m. This led to a decrease of the Z value from 28.6 Ω to 3.5 Ω for the first model (Fig. 3). With increasing of w/t_1 ratio, the difference Z between the first and second models decreased from 2.1 Ω to 0.2 Ω due to the decrease of L .

The positive effect associated with the increase in capacitance and the decrease in the inductance takes place with serious drawbacks in the terms of mass, dimensions, and cost of the PBB design. So, the increase of the ratio of w/t_1 from 2 to 200 mm will increase the weight of the structure by 205% (from 316 g to 650 g, per 1 m of length), and the total area of cross-section ($w \times (2 \times t_1 + t_2)$) will increase by 250%

(from 120 mm^2 to 300 mm^2). This is due to the tenfold increase of the dielectric thickness t_2 . These drawbacks can be significant in developing the overall design of the device. Thus, it is necessary to find the optimal aspect ratio that meets the design requirements of the device as a whole, and consider options for changing the shape of the cross-section and the dielectric constant of insulating materials.

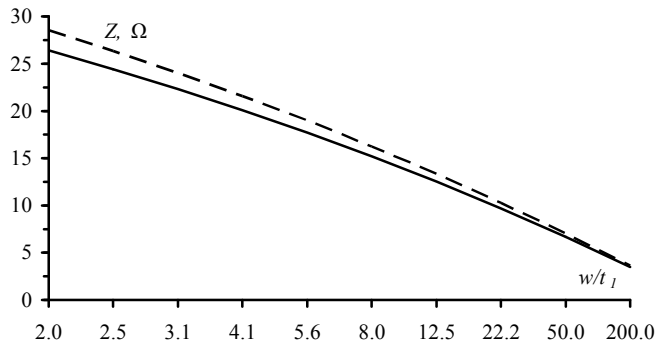


Fig. 3. Dependence of the characteristic impedance (Z, Ω) on the ratio w/t_1 for the first (—) and second (---) models

B. Changing of permittivity

Calculating of the L and C values was performed during ϵ_r changing. For this purpose maximum ($w/t_1=200$) and minimum ($w/t_1=2$) values of w/t_1 are selected for first and second PBB model structure. Analysis of the dependency shows that when increasing ϵ_r from 1 to 10, C value rises for $w/t_1=200$ (from 477.8–491.6 pF/m to 4360–4461 pF/m) by a factor of 1.45 faster than for $w/t_1=2$ (from 72.7–74.4 pF/m to 460.6–471.5 pF/m). The L value, during ϵ_r rising for $w/t_1=200$ (23.3–25.2 nH/m) and for $w/t_1=2$ (153–177.3 nH/m) is almost permanent for both variants, appropriately. Thus, the capacitance component is significantly changing under ϵ_r increasing, which significantly influences Z (Fig. 4).

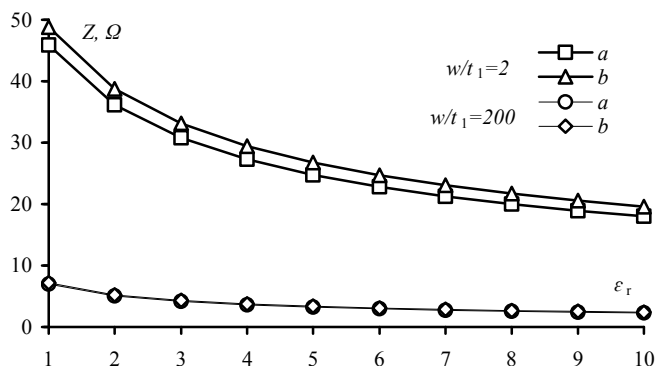


Fig. 4. Dependence of characteristic impedance (Z, Ω) on permittivity (ϵ_r)

Fig.4 shows that value of Z is almost equally decreased from 46–48.8 Ω to 18–20 Ω for $w/t_1=2$ and from 7–7.2 Ω to 2.3–2.4 Ω for $w/t_1=200$ for both model variants that is a positive effect during PBB model creating.

C. Rounding the corners of conductors

The above-described models have corners where the charge density is higher than between them. It can result in premature voltage breakdown via dielectric around the PBB. Rounding of PBB's conductor corners with taking into account saving of conductor cross-section area was performed ($S=50 \text{ mm}^2$).

Maximum rounding radius $r=t_1/2$ was selected (Fig. 5). The L and C values were calculated; and based on the results the Z value was calculated under permittivity value ϵ_r changing.

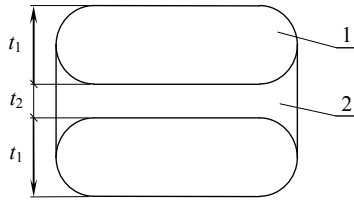


Fig. 5. Cross-section with rounded corners

The C value dependency analysis with rounded corners was performed. With increasing ϵ_r from 1 to 10 the C value also linearly rise. However, for rounded corners the C value insignificantly decreases by 12–4.8 pF/m for $w/t_1=200$ and by 12.5–2.6 pF/m for $w/t_1=2$, and L value increases by 0.6 nH/m (23.9 nH/m) and 32 nH/m (185 nH/m), appropriately, in comparison with the right angle. The Z value dependence on ϵ_r was calculated (Fig. 6).

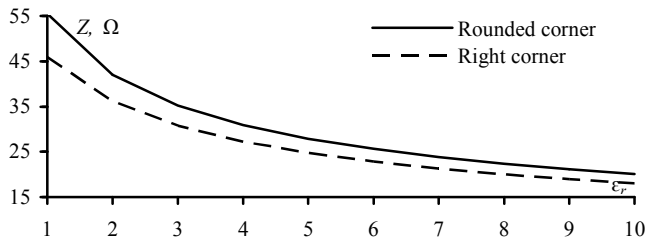


Fig. 6. Dependence of Z on permittivity ϵ_r

Fig. 6 shows that Z value will rise on 10 Ω (up to 55 Ω) under rounding of the corner edge of every PBB conductor, and will gradually fall to 20 Ω under growing of ϵ_r from 1 to 10. Furthermore, PBB mass is almost permanent in comparison with the first and second models. However, technological process of structure creation will be more complex.

III. CHANGING THE CROSS-SECTION OF BUS BAR

A change in the shape of the PBB cross-section (Fig. 7) with the unchanged area of each conductor ($S=50 \text{ mm}^2$) has been performed. The L , C and Z parameters are calculated, for each PBB, the results are summarized in Table I.

From Table I, it follows that as w/t_1 increases by a factor of 100, the values of L and Z decrease significantly and C increases, which is a positive effect of the PBB. With an increase of w/t_1 of the cross-section with rounded corners (Fig. 5), the per-unit-length capacity increases significantly (by a factor of 2) and the structural mass practically does not change, and the electrical strength of the structure also increases. However, the technological process of manufacturing a similar PBB becomes more complicated. The cross-sectional shapes shown in Fig. 7, *a, f*, are appropriate for their execution with a relatively low value of w/t_1 and have a characteristic impedance for $w/t_1=2$, which is half as much compared to the cross-sectional shape shown in Fig. 1, while the mass of the structure is insignificantly (by 10 g) less (306 g). However, with an increase in w/t_1 to 200 there is an

increase in the per-unit-length capacitance and a decrease in inductance, which decreases Z . For coaxial cross-sectional shapes (Fig. 7, *b, d, e*) the L , C , Z parameters turned out to be the best with the minimum mass and dimensions, and an increase in w/t_1 will reduce L and increase C .

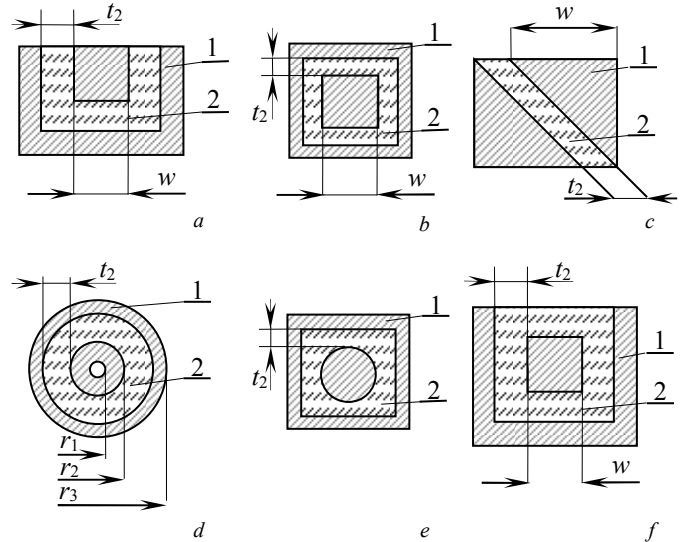


Fig. 7. Various cross-sections of the PBB

TABLE I
PARAMETERS OF THE PBB OF VARIOUS CROSS-SECTIONS

Cross-section	w/t_1	C , pF/m	L , nH/m	Z , Ω
	2	219	153	26.4
	200	1938	23.3	3.5
	2	217.5	177.3	28.6
	200	1927	25.2	3.6
	2	458	185	20.1
	200	4451.8	24	2.3
	1	623.8	46.7	11.1
	100	8452	5.7	0.8
	1	271.6	143.9	23
	1	511.7	89.4	13.2
	100	1489.6	31	4.6
	1	463.3	92.8	14.2
	100	1451.7	31.6	4.7
	–	595.2	80.4	11.6
	–	545.6	82.9	12.3

An increase in the radius of the conductors from Fig. 7 *d*. With the increase of the radius, the cross-section area of every conductor, equal $S=50 \text{ mm}^2$, was taken into account, which resulted in decreasing of thickness and increasing of the radius of every conductor, an air filling has arisen inside the central conductor. The parameters (Table II) are calculated, where it can be seen that the increase in the radius of the coaxial conductor produces a slight change in the per unit length parameters.

TABLE II
PARAMETERS OF THE PBB WITH THE CHANGE OF THE INTERNAL AND
EXTERNAL RADIUS OF THE CONDUCTOR FROM FIG. 7 d

r_1 , mm	r_2 , mm	r_3 , mm	C , pF/m	L , nH/m	Z , Ω
0.25	3.99	7.2	533.71	84.44	12.58
0.5	4.02	7.22	536.08	84.04	12.52
1	4.11	7.3	545.86	82.49	12.29
1.5	4.26	7.43	561.78	80.12	11.94
2	4.46	7.6	583.26	77.13	11.49
2.5	4.71	7.81	609.44	73.77	11.00
3	4.99	8.05	639.72	70.23	10.48

The cross-section shown in Fig. 7 b is interesting in terms of finding the optimal geometric parameters. It has a small per-unit-length inductance ($L=46.7$ nH/m) and a high per-unit-length capacitance ($C=623.75$ pF/m), for $w/t_1=2$, and the mass of the structure is 366 g. With an increase in w/t_1 by a factor of 100, L decreases to 5.7 nH/m; and C increases to 8.5 nF/m. The shape of the cross-section is quite simple for analysis, since it represents a known shielded stripline, but such a structure is difficult to manufacture. Meanwhile, it is advisable to analyse it with rounded corners and find its optimal parameters.

IV. CONCLUSION

The calculation of the parameters of the PBB for various forms of the cross-section (for an area equal to 50 mm²) and the dielectric constant of the insulating material is performed. The results of calculations of the parameters and their dependence on the thickness, width, and shape of the conductors are presented. The analysis of mass, dimensions and technological possibilities of PBB manufacturing is carried out. The optimal parameters of the PBB cross-section are determined, according to the criteria of the minimum inductance and characteristic impedance.

REFERENCES

- [1] E. Clavel, J. Roudet, J.L. Schanen, A. Foutanet, "Influence of the cabling geometry on paralleled diodes in a high power rectifier," *IEEE Conf. Record of the Industry Applications Conference*, vol. , pp. 993–998, 6–10, Oct. 1996.
- [2] W. Huiqing, L. Jun, Z. Xuhui, W. Xuhui. "Electric vehicle drive inverters simulation considering parasitic parameters," *13th Power Electronics and Motion Control Conference*, pp. 417–421, 1–3, Sept. 2008.
- [3] F. Denk, C. Simon, M. Heidinger, R. Kling, W. Heering, "Compact highly efficient 3-kW MHz inverter based on smt sic mosfets," *Proc. of Int. Exhibition and Conf. for Power Electronics, Intelligent Motion, Renewable Energy and Energy Management*, pp. 1–5, 16–18, May 2017.
- [4] M. Youssef, G. Antonini, E. Clavel, J. Roudet, S. Cristina, A. Orlandi, "Conducted and radiated EMI characterisation of power electronics converter", *Proc. of the IEEE Int. Symp. on Industrial Electronics*, vol. 1 pp. 207–211, 7–11, July 1997.
- [5] W. Zhang, M.T. Zhang, F.C. Lee, J. Roudet, E. Clavel, "Conducted EMI analysis of a boost PFC circuit", *Conf. Proc. Applied Power Electronics Conference and Exposition*, vol. 1, pp. 223–229, 27–27, Feb. 1997.
- [6] M.T. Zhang, R. Watson, F.C. Lee, J. Roudet, J.-L. Schanen, E. Clavel, "Characterization and analysis of electromagnetic interference in a high frequency AC distributed power system", *Annual IEEE Power Electronics Specialists Conf.*, vol. 2, pp. 1956–1960, 23–27, June 1996.
- [7] M. Stibgen. "Applying laminated busbars to enhance DC power distribution systems", *26th Annual Int. telecommunications Energy Conference (INTELEC)*, pp.537–541, 19–23, Sept. 2004.

- [8] Y. Zhenyang, W. Shishan, S. Zheng, B.-L. Lee, "The reviews of integrated EMI filters applied in power electronic system", *Asia-Pacific Symp. on Electromagn. Compat. (APEMC)*, pp. 227–230, 26–29, May 2015.
- [9] J. Stewart, J. Neely, J. Delhotal, J. Flicker, "DC link bus design for high frequency, high temperature converters", *IEEE Applied Power Electronics Conf. and Exposition (APEC)*, pp. 809–815, 26–30, March 2017.
- [10] J. Wang, B. Yang, J. Zhao, Y. Deng, X. He, X. Zhixin, "Development of a compact 750KVA three-phase NPC three-level universal inverter module with specifically designed busbar", *Applied Power Electronics Conf. and Exposition (APEC)*, pp. 1266–1271, 21–25, Feb. 2010.
- [11] M. Youssef, G. Antonini, E. Clavel, J. Roudet, S. Cristina, A. Orlandi, "Conducted and radiated EMI characterisation of power electronics converter", *Proc. of the IEEE Int. Symp. on Industrial Electronics*, vol. 1, pp. 201–211, 7–11, July 1997.
- [12] X. Zhang, H. Zhang, R.-W. Yu, G.-J. Tan, "Planar bus bar optimum design in high-power converters based on FEM analysis", *IEEE Int.Symp. on Power Electronics for Distributed Generation Systems (PEDG)*, pp. 167–170, 16–18, June 2010.
- [13] H.K. Shashikiran, "Magnetic modelling to capture geometry based impedance matrix for Busbar", *IEEE Int. Transportation Electrification Conference (ITEC)*, pp. 1–3, 27–29, Aug. 2015.
- [14] I. Popa, A.I. Dolan, "Numerical modeling of DC busbar contacts", *Int. Conf. on Optimization of Electrical and Electronic Equipment (OPTIM)*, pp. 188–193, 24–26, May 2012.
- [15] L. Smirnova, R. Juntunen, K. Murashko, T. Musikka, J. Pyrhönen, "Thermal Analysis of the Laminated Busbar System of a Multilevel Converter", *IEEE Trans. on Power Electronics*, vol. 31, pp. 1479–1488, Feb. 2016.
- [16] H. Liang, R. Wang, L. Bao, H. Wang, J. You, "Research on the distribution thermal FEM model for an enclosed isolated phase bus-bar in short-circuit condition", *IEEE Holm Conf. on Electrical Contacts*, pp. 55–58, 10–13, Sept. 2017.
- [17] Jm. Guichon, J. Aime, JI. Schanen, C. Martin, J. Roudet, E. Clavel, M. Arpilliere, R. Pasterczyk, Y. Le Floch, "Busbar Design: How to Spare Nanohenries?", *Industry Applications Conf.*, pp. 1865–1869, 8–12, Oct. 2006.
- [18] M. Ehrlich, L.O. Fichte, M. Luer "Electrical properties and magnetic fields of a coaxial bus bar", *Proc. Asia-Pacific Conf. on Environmental Electromagnetics*, pp. 11–16, 7–7 May 2000.
- [19] V.V. Dvirnyi, V.V. Eremenco, G.V. Dvirnyi, "Reduction of spacecraft harness mass", *Vestnik SibGAU*, vol. 16, pp. 658–663.
- [20] S.P. Kuksenko, A.M. Zabolockij, A.O. Melkozerov, T.R. Gazizov, "Novye vozmozhnosti sistemy modelirovaniya ehlektromagnitnoj sovместimosti TALGAT", *Doklady TUSUR*, Vol. 36, № 2, pp. 45–50, 2015.



Stanislav Ternov was born in 1995. He graduated from the Tomsk State University of Control Systems and Radioelectronics (TUSUR) in 2016. He is currently working as an engineer in the Research Laboratory of «Safety and Electromagnetic Compatibility of Radioelectronic Facilities» (SECRF) of TUSUR. Currently, He is a master of TUSUR.



Alexander V. Demakov was born in 1994. He has been studied at the TUSUR since 2012. Currently he works in the research laboratory «SECRF» of TUSUR.



Maxim E. Komnatov (S'15, M'17) was born in 1987. He graduated from the TUSUR in 2013. He defended his Ph.D. thesis. Currently, he works as a senior researcher at the Research Laboratory «SECRF» and an associate professor at the Department of TUSUR. The field of scientific interests is measurements and tests on EMC. M.E. Komnatov is the author of 79 scientific works.